

L. D. Roelofs,^{a)} Robert L. Park, and T. L. Einstein*Department of Physics and Astronomy, University of Maryland, College Park, Maryland 20742*

(Received 20 October 1978; accepted 19 December 1978)

We present a Monte Carlo study of the adlayer-induced LEED beams in a representative order-disorder transition. Calculations of the widths of fractional order beams indicate that, as seen in recent experimental work on the O/Ni(111) system, these widths rise sharply and suddenly above T_c . Furthermore the slope of this rise provides a sensitive probe of the adatom-adatom interactions. The increase in the width results from the existence of ordered domains above T_c , and has not been previously discussed since prior calculations have concentrated on beam intensities. We further derive a functional relation between the window approach used in simulations of order-disorder transitions and the instrument response function approach of the experimentalist, to detail the effect of the LEED apparatus on the profile of the extra beams.

PACS numbers: 61.14.Hg, 64.60.Cn, 82.65.My, 02.50.Ng

I. INTRODUCTION

The adsorption of simple gases on single-crystal metal surfaces frequently takes the form of ordered two-dimensional crystals in registry¹ with the substrate net. Until recently, the emphasis in low-energy electron diffraction (LEED) studies of adsorption has been to deduce the structural details of these static ordered overlayers. Such structures often exhibit order-disorder transitions,² and there has been increasing interest in using LEED to follow these phase changes in the adsorbed layers.

Since the adatoms are confined to an array of identical sites, a lattice gas model is commonly adopted. This model generally requires use of Monte Carlo techniques to make progress. The most straightforward specific problem is a square lattice substrate with a $c(2 \times 2)$ overlayer produced by nearest-neighbor repulsions. In the solution it is not enough to characterize the nature of the phase transition, say by finding the temperature dependence of the pair correlation function. One must also consider the limitations of the LEED instrument to determine what information is accessible to measurements.

Doyen *et al.*³ have broached these problems and shown their importance. Their early treatment, however, obscures much of the physics of the disordering process and neglects the shape of the adlayer-induced LEED spots, with unsatisfactory consequences. In this paper we re-examine their approach. In Sec. II, we show for the first time how the well-known instrument response function approach used by experimentalists relates to the window function or lattice truncation viewpoint of theorists. This understanding is crucial to obtaining quantitative information from LEED spots. Section III recounts the possible mechanisms underpinning the overlayer disordering process and discusses how the instrument response limits one's ability to distinguish between them experimentally. Application is made to Kortan's new data for O/Ni(111).⁴ The chief conclusion is that calculating the LEED intensity only at the half-order points, i.e., the exact center of the adlayer-induced spots, misses much of the

physics underlying spot broadening and splitting. In the limit of a "perfect" instrument, such a calculation at the $(\frac{1}{2} \frac{1}{2})$ point reduces to the famous Onsager curve for the magnetization of the zero-field Ising model; this approach gives no information about the antiphase ordered islands that exist above T_c and are responsible for the broadening and splitting.⁵ In Sec. IV we report our own Monte Carlo results, emphasizing the need to perform calculations over a substantial region of the surface Brillouin zone surrounding the LEED spot. As others recently recognized,⁶ careful analysis of extra-spot widths provides a practical means to probe inter-adatom interactions.

II. RELATIONSHIP BETWEEN THE LEED INSTRUMENT RESPONSE FUNCTION AND THE LATTICE WINDOW FUNCTION

A variety of factors, including finite source and detector extension, beam nonmonochromaticity and divergence, limit the range over which a LEED instrument can probe correlations.⁷ This range is typically 40–150 Å.

Quantitatively, one introduces the instrument response function, $T(k)$, defined by:

$$I_{\text{meas}}(k) = T(k) * I_0(k), \quad (1)$$

where $*$ denotes the convolution product:

$$g_1(x) * g_2(\pm x) \equiv \int dy g_1(y) g_2[\pm(x - y)],$$

$I_0(k)$ is the diffracted intensity at momentum transfer k , and $I_{\text{meas}}(k)$ is the intensity measured by the instrument. T depends on other parameters such as the incidence angle, energy of electrons, and the indices of the observed beam.

In calculations of the intensity patterns from model systems, the effect of the instrument is introduced crudely by describing the measured intensity as arising from a region of the surface of some characteristic size,^{3,8,9} which is equivalent to introducing a beam coherence zone. We derive the equation relating this zone to the instrument response function defined in Eq. (1).

The intensity pattern that would be seen by a perfect instrument is the Fourier transform of the convolution square of the surface¹⁰

$$I_0(\mathbf{k}) = \mathcal{F}\{\ell(\mathbf{r}) * \ell(-\mathbf{r})\} \\ = 1/\sqrt{2\pi} \int_{-\infty}^{\infty} d\mathbf{r} e^{-i\mathbf{k}\cdot\mathbf{r}} [\ell(\mathbf{r}) * \ell(-\mathbf{r})], \quad (2)$$

where $\ell(\mathbf{r})$ denotes the surface scattering function, e.g., a net of delta functions. We then obtain the measured intensity using Eq. (1).

Using a finite lattice to model the instrumental limitations is equivalent to truncating the lattice by multiplying $\ell(\mathbf{r})$ by a window function $c(\mathbf{r})$:

$$\ell_t(\mathbf{r}) = c(\mathbf{r})\ell(\mathbf{r}). \quad (3)$$

The truncated lattice is typically square, i.e. $Ma \times Ma$, where a is the lattice constant. This window function is, explicitly,

$$c(\mathbf{r}) = \begin{cases} 1 & |r_x| \text{ and } |r_y| \leq Ma/2 \\ 0 & \text{otherwise,} \end{cases} \quad (4)$$

The intensity arising from this truncated lattice alone is

$$I_{\text{calc}}(\mathbf{k}) = |\mathcal{F}\{\ell_t(\mathbf{r})\}|^2. \quad (5)$$

There is no functional relationship between $T(\mathbf{k})$ in Eq. (1) and $c(\mathbf{r})$ implicitly in Eq. (5) that will allow $I_{\text{calc}} = I_{\text{meas}}$, since no single part of the lattice gives full information on the whole. However, $c(\mathbf{r})$ can be treated as a movable window which can scan the whole lattice. By averaging over all placements of the center, \mathbf{r}_0 , of the window, we obtain

$$I_{\text{calc}} = \int d\mathbf{r}_0 |\mathcal{F}\{\ell(\mathbf{r})c(\mathbf{r} - \mathbf{r}_0)\}|^2. \quad (6)$$

The convolution theorem gives

$$I_{\text{calc}} = \int d\mathbf{r}_0 \mathcal{F}\{[\ell(\mathbf{r})c(\mathbf{r} - \mathbf{r}_0)] * [\ell(-\mathbf{r})c(-\mathbf{r} + \mathbf{r}_0)]\}. \quad (7)$$

After changing the order of integration, we eventually find

$$I_{\text{calc}} = \mathcal{F}\{ \int d\mathbf{y} \ell(\mathbf{r} + \mathbf{y})\ell(\mathbf{y}) \\ \times \int d\mathbf{r}_0 c(\mathbf{r} + \mathbf{y} - \mathbf{r}_0)c(\mathbf{y} - \mathbf{r}_0) \}. \quad (8)$$

A change of variables and another application of the convolution theorem finally yield

$$I_{\text{calc}}(\mathbf{k}) = I_0(\mathbf{k}) * T_{\text{calc}}(\mathbf{k}), \quad (9)$$

where

$$T_{\text{calc}}(\mathbf{k}) = \mathcal{F}\{c(\mathbf{r}) * c(-\mathbf{r})\} = |\mathcal{F}\{c(\mathbf{r})\}|^2. \quad (9)$$

Obviously, the instrument response function is positive definite, as expected on physical grounds. Comparison of Eq. (9) and (1) indicates that the instrument function is the Fourier transform of the convolution square of the window function. For example the square window of Eq. (4) gives an instrument response of

$$T_{\text{calc}}(\underline{k}) = \frac{\sin^2(Ma k_x/2) \sin^2(Ma k_y/2)}{(k_x/2)^2 (k_y/2)^2}. \quad (10)$$

Note, however, that our derivation holds for any window function not just the square box of Eq. (4). We note that this approach would be inappropriate for simulation studies of adatom island shape, which is probed by beam shape,¹⁸ since

T_{calc} is not circularly symmetric. Furthermore due to the sharp truncation, T_{calc} has nonphysical oscillations which give rise to side lobes on sharp beams.

In short, Eq. (9) relates quantitatively and uniquely the instrument response, which can be measured with considerable precision,¹¹ to a window through which the lattice is viewed. The complete equivalency of these two viewpoints has the important consequence of giving an explicit solution to the problem of the (real-space) range over which a LEED instrument with known response function can probe the adatom pair correlation function. In other words, the many uncertainties underlying a LEED experiment can be folded into one \mathbf{k} -dependent instrument response function which can be precisely measured. The Fourier transform of this function, called the transfer function, has no special physical significance, and the transfer [function] width is certainly not the limit of the range of the LEED measurement, as has sometimes been implied. Rather, one must determine the unique window function whose convolution square is the transfer function, the deconvolution being a well-defined mathematical procedure in this case.¹² It is this window function which multiplies the lattice scattering function to determine the effective scattering function one actually measures. Thus, its specific shape (width, tails, azimuthal dependence, etc.) must be well understood to obtain detailed quantitative information from LEED spots. We emphasize that the window function encompasses *all* the sources of "incoherence" in the experiment and that it is thus fruitless to speak (separately) of some huge unmeasurable electron coherence width over which the lattice is in principle probed, with subsequent blurring by the specific instrument. As specific examples, if T (in one direction in \mathbf{k} -space) is a Gaussian of width W , the associated window function (in real space) is indeed also a Gaussian but of width $1/\sqrt{2} W$, rather than the usually-quoted $1/W$. If $T(\mathbf{k})$ is a Lorentzian of width W , then $c(x)$ is the modified Bessel function $K_0(W|x|)$, which has width $1/W$. These numerical details must be included in quantitative measurements of island size and of substrate perfection. In the general case the second moment of the convolution square of an even, normalized function is twice the second moment of the function itself. On this basis, the width of the window function will always be $1/\sqrt{2}$ of the width of the Fourier transform of the instrument response function.

III. ORDER-DISORDER TRANSITIONS IN LATTICE GAS MODELS

The extra LEED beams produced by adatom superlattices display a variety of changes, including broadening, splitting, and decreasing intensity, as the system is heated through its adlayer order-disorder transition. These changes constitute a sensitive probe of the disordering process, since the various changes may be associated with various disorder types, but careful treatment of the LEED instrument is required. We assume a lattice gas model and for specificity consider a $c(2 \times 2)$ overlayer on a square net face.

In Bragg-Williams disorder, or disorder of the first kind, the disorder takes the form of point imperfections. The surface may be thought of as a checkerboard with say the "black squares" being preferred at $T = 0$. At finite temperature,

however, a few of the "red squares" are occupied due to random thermal motion. Estrup¹³ showed that as the order parameter, α , decreases, the *width* of the half-order peak is unchanged while its *intensity* decreases as the square of α and a uniform background increases as $(1 - \alpha^2)$. Unless $\alpha = 0$, long-range order is preserved.

In disorder of the second kind, long-range order is lost, but considerable short-range order persists in the form of ordered domains. With increasing disorder, the average size of the domains decreases, and the extra beams broaden.

In a subclassification of disorder of the second kind, the domains have a narrow distribution of sizes. In treating this situation Pendry¹⁴ stated incorrectly that the extra LEED beams are extinguished due to phase cancellation when the size of the domains is such that many fit into the coherence zone. Houston and Park⁵ have shown (in one dimension) that in fact the extra beams are split by $2\pi/N_0a$ ¹⁵ where N_0a is the average domain size: the width of the split beams is inversely proportional to the width of the domain size distribution. (More arcane types of adatom disorder involve multiple adlayers¹⁶ or substrate reconstruction¹⁷.)

The LEED instrument confuses these classifications in two ways. If the instrument response function dominates the width of the extra beams, the beam broadening will be difficult to detect; the experimenter then cannot distinguish between disorders of the first and second kind. If the splitting in the subclass of disorder of the second kind is small, it will be smeared out by convolution with the instrument response. Both effects are due to the limited range over which correlations are probed.

Moreover, these types of disorder are ideal in that a given transition may show successively, and perhaps even simultaneously if the surface is very nonuniform, evidence for different sorts of disorder. For example Kortan *et al.* have obtained new data for O/Ni(111), which exhibits a reversible order-disorder transition, with $T_c \approx 400$ K.⁴ The break in the width plot indicates, since up to that point no increase in beam width above the minimum width determined by the instrument has occurred, that the transition begins with Bragg-Williams disorder, and near T_c (the inflection point of the intensity plot) changes to disorder of the second type with concomitant beam broadening. We expect this rather sharp change in the type of disordering to be an important probe of the interadatom interactions, since the formation of small ordered domains must depend strongly on the sign and magnitude of the next nearest neighbor and possibly on three-adatom interactions.¹⁸

IV. MONTE CARLO RESULTS

We have begun a series of Monte Carlo calculations to study, via simulated LEED patterns, the participation of different types of disorder in a given transition. Thus we can probe the underlying role of the interadatom interactions. Our routine is in many respects similar to that of others.¹⁹ However to compare to experimental measurements of half-order beam widths it is not sufficient to calculate the intensity just at the half-order point as previously done.^{3,8,9} Rather we calculate the intensity pattern in the surface Brillouin zone, along the $\langle 11 \rangle$ and sometimes the $\langle 10 \rangle$ directions passing through the

half-order point (the center of the first quadrant for our $c(2 \times 2)$ structures), thereby also obtaining information on the beam profiles. For equilibration diagnostic parameters we use the hopping rate, the nearest-neighbor and next-nearest-neighbor correlation functions, the calculated intensity at the half-order point, and the total number of adatom hops.

We use relation Eq. (9) to determine an appropriate lattice size. The common choice of a 30×30 site array corresponds to a lattice with the dimensions of the window width, ~ 100 Å. *This choice is not adequate.* A realistic instrument response does not correspond to a window which cuts off precipitously at 100 Å; rather there are tails which allow information to be obtained over somewhat longer range, albeit with decreasing signal-to-noise. We thus chose a 50×50 site array and broadened with a Gaussian to obtain a window width of 100 Å. This treatment results in a realistic instrument response function (of controllable width) which also avoids nonphysical truncation-induced oscillations. There are also statistical finite-size and boundary-condition effects; these are substantially reduced in our larger lattice.²⁰

Doyen *et al.* claimed that random lattices equilibrate in the time required for each adatom to make five hops.³ We find that longer times, typically 15 hops/adatom, are necessary near T_c (see Fig. 1). Our various diagnostic parameters showed fluctuations on a time scale that was the time required for each adatom to make roughly five hops (Fig. 1). This observation establishes the time scale over which averaging of the LEED pattern must be performed. We typically allowed approximately one hop/adatom between calculations of the diffraction pattern and averaged over five or six such patterns.

Our data was obtained from an initial array that was either perfectly ordered (annealed) or that had equilibrated at a lower temperature. This procedure was necessary, since the

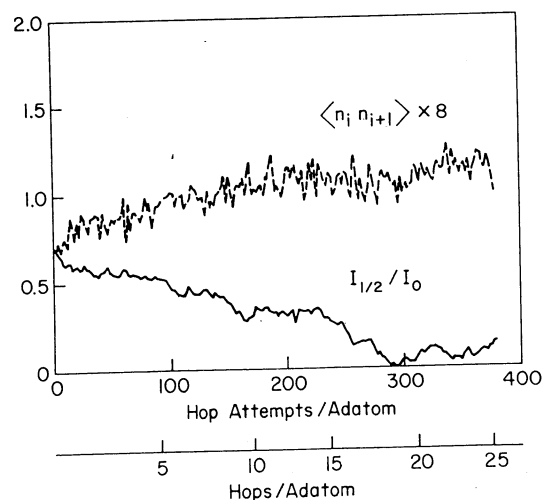


FIG. 1. Example of the equilibration of a half monolayer of adatoms on a square lattice in the Monte Carlo calculation. The solid line displays the intensity at the half-order point (normalized by the integer-order beam intensity) while the broken line gives the mean number of nearest neighbors per adatom, which for this coverage and symmetry is eight times the nearest neighbor pair correlation function. Both are plotted versus two abscissae, the number of hop attempts per adatom and the actual number of hops made per adatom. The ratio of actual hops to attempted hops decreases as equilibrium is approached. The lattice was 50×50 sites, at temperature $T = 1.08T_c$, with $E_2/E_1 = -0.3$.

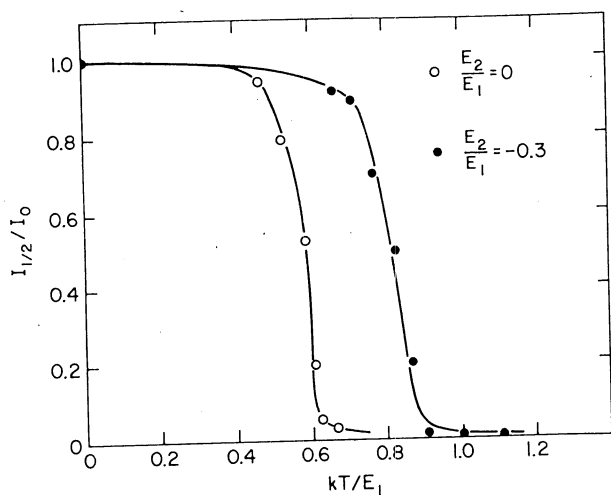


FIG. 2. Intensity of the extra beams in simulated LEED patterns versus temperature obtained by Monte Carlo calculations. Solid circles: $E_2/E_1 = -0.3$; open circles: $E_2/E_1 = 0$. These plots give one relation among T_c , E_1 , and E_2 .

width calculations are very sensitive to 'frozen in' domain boundaries that frequently occur when a random lattice is allowed to relax at low temperature, and seems to correspond to the experimental conditions more closely than the use of an initially random lattice. Metastable domain walls were also noted by Williams *et al.*⁸ They unaccountably chose to omit such cases from their averages, thus missing the interesting domain fluctuations near T_c ; their calculated curves consequently lack the tails of the experimental data above T_c .

Figure 2 shows the variation of the intensity at the half-order point as a function of temperature for two different values of the ratio E_2/E_1 , where E_1 and E_2 are the nearest- and next-nearest-neighbor interactions, respectively. The coverage is $1/2$ and E_1 is repulsive to give the $c(2 \times 2)$ structures. The transition temperature is not well defined for a finite lattice. Previous workers have used the inflection point of the half-order intensity curve.²¹ A more meaningful determination is based on the maximum in the specific heat,

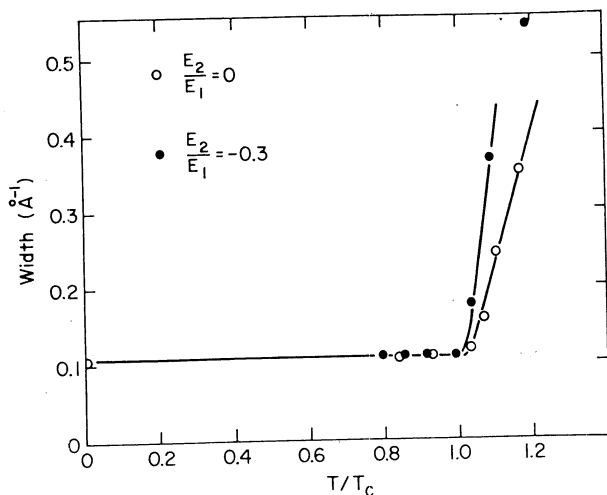


FIG. 3. Width (FWHM of Gaussian fitted to beam) of the extra beam in simulated LEED patterns as a function of temperature obtained by Monte Carlo calculations. Solid circles: $E_2/E_1 = -0.3$; open circles: $E_2/E_1 = 0$. Note that temperature is normalized by T_c ; plots such as these may be used to determine the ratio E_2/E_1 in comparisons with experimental data.

which corresponds to the inflection point of the *internal energy* curve.²⁰ There is, however, a more physical and more precise method for determining T_c based on the width of the LEED beams.

Figure 3 shows the width calculations for the overlayer peak as a function of T/T_c for the two values of the ratio E_2/E_1 . These results show a remarkably sharp break in the beam width, which is similar to the experimental results (Fig. 4 of Ref. 4) for O/Ni(111). The break constitutes the more precise measure of T_c since the temperature at which the beam begins to broaden, i.e. the point of the initial deviation of the width curve from the instrumental widths, coincides with the vanishing of long-range order (which marks the true transition point). The transition temperatures obtained in this fashion are in excellent agreement with those found from statistical mechanics calculations.²²

Since the slope of the width curve above T_c is rather sensitively dependent on the ratio E_2/E_1 , this measurement together with a transition temperature measurement (as in Fig. 2) determines E_2 as well as E_1 . E_2 can in principle also be determined from the coverage dependence of T_c ,²³ but since absolute coverage measurements are tricky, an independent measurement of E_2 is very useful. To better characterize interatom interactions, the next step will be to add short-range three-atom forces. These interactions lead to asymmetries in the phase diagram about half-monolayer coverage,²⁴ renormalize E_1 and E_2 ,²⁵ and usually outweigh more distant pair interactions.²⁵

ACKNOWLEDGEMENTS

We would like to thank W. T. Elam and J. Cavallo for programming assistance, A. R. Kortan for frequent discussions of his results, and G.-C. Wang for sending us a copy of her thesis.

Computing facilities and time were provided by the Computer Science Center of the University of Maryland. We are grateful to the National Science Foundation for supporting this work (Grant No. DMR 76-84576-A01).

^a)From a dissertation to be submitted to the Graduate School, University of Maryland by Lyle D. Roelofs in partial fulfillment of the requirements for the Ph.D. degree in physics.

¹The overlayer is said to be "simply related" to the substrate net in these cases. See R. L. Park and H. H. Madden, *Surf. Sci.* **11**, 188 (1968).

²See for example: G. Ertl and D. Schillinger, *J. Chem. Phys.* **66**, 2569 (1977); J. C. Buchholz and M. G. Lagally, *Phys. Rev. Lett.* **35**, 442 (1975); A. U. MacRae, *Surf. Sci.* **1**, 319 (1964); P. J. Estrup, *Phys. Today* **28**, 33 (April 1975).

³C. Doyen, G. Ertl, and M. Plancher, *J. Chem. Phys.* **62**, 2957 (1975).

⁴A. R. Kortan, P. I. Cohen, and R. L. Park, *J. Vac. Sci. Technol.* **16**, 541 (1979).

⁵R. L. Park and J. E. Houston, *Surf. Sci.* **18**, 213 (1969); J. E. Houston and R. L. Park, *Surf. Sci.* **21**, 209 (1970).

⁶J. C. Buchholz and M. G. Lagally, *Phys. Rev. Lett.* **35**, 442 (1975); M. G. Lagally, G.-C. Wang, and T.-M. Lu, invited paper at Third Internat'l. Summer Inst. in Surf. Sci., Milwaukee, 1977; *CRC Crit. Rev. Solid State Mater. Sci.* **7**, 233 (1978). LEED spot width calculations, as a function of coverage only, are mentioned by G. Ertl and D. Schillinger, *J. Chem. Phys.* **66**, 2569 (1977). They do not exploit these calculations to determine interaction energies.

⁷R. L. Park, J. E. Houston, and D. G. Schreiner, *Rev. Sci. Instrum.* **42**, 60

- (1971).
- ⁸E. D. Williams, S. L. Cunningham, and W. H. Weinberg, *J. Chem. Phys.* **68**, 4688 (1978).
- ⁹W. J. Ching, D. L. Huber, M. Fishkis, and M. G. Lagally, *J. Vac. Sci. Technol.* **15**, 653 (1978).
- ¹⁰A. Guinier, *X-Ray Diffraction* (Freeman, San Francisco, 1963), Chap. 2.
- ¹¹G.-C. Wang and M. G. Lagally, *Surf. Sci.* (to be published).
- ¹²R. Hosemann and J. N. Bagchi, *Direct Analysis of Diffraction by Matter* (North-Holland, Amsterdam, 1962), Chaps. 2 and 4.
- ¹³P. J. Estrup in *The Structure and Chemistry of Solid Surfaces*, edited by G. A. Somorjai (Wiley, New York, 1969).
- ¹⁴J. B. Pendry, *Low Energy Electron Diffraction* (Academic, London and New York, 1974), p. 236.
- ¹⁵The magnitude of the splitting is easily understood when it is realized that the period of the structure is $2N\phi a$ and the beam at $ka = \pi$ is cancelled by the occurrence of antiphase domains.
- ¹⁶See for example: F. Jona, K. O. Legg, D. H. Shih, D. W. Jepsen and P. M. Marcus, *Phys. Rev. Lett.* **40**, 1466 (1978); T. Edmonds and R. C. Pitkethly, *Surf. Sci.* **15**, 137 (1969).
- ¹⁷R. A. Barker and P. J. Estrup, *Phys. Rev. Lett.* **41**, 1307 (1978).
- ¹⁸T. L. Einstein, *Surf. Sci.* **82**, xxx (1979); *CRC Crit. Rev. Solid State Mater. Sci.* **7**, 261 (1978).
- ¹⁹See for example: G. Ertl and J. Kuppers, *Surf. Sci.* **21**, 61 (1970); and Ref. 8. We do not allow the long-range hops used in Ref. 8.
- ²⁰A treatment of these effects in an analogous Ising problem is given by D. P. Landau, *Phys. Rev. B* **13**, 2997 (1976).
- ²¹J. Behm, K. Christmann and G. Ertl, *Solid State Commun.* **25**, 763 (1978).
- ²²C. Fan and F. Y. Wu, *Phys. Rev.* **179**, 560 (1969); N. W. Dalton and D. W. Wood, *J. Math. Phys.* **10**, 1271 (1969).
- ²³T. M. Lu, G.-C. Wang, and M. G. Lagally, *Phys. Rev. Lett.* **39**, 411 (1977).
- ²⁴W. Y. Ching, D. L. Huber, M. G. Lagally and G.-C. Wang, *Surf. Sci.* **77**, 550 (1978).
- ²⁵T. L. Einstein, U. of Maryland Physics Paper No. 79-106 (submitted *Surf. Sci.*).